Electro-Copolymerization of Acrylonitrile and Methyl Acrylate onto Graphite Fibers

J. CHANG, J. P. BELL, and S. SHKOLNIK, *Polymer Science Program, University of Connecticut, Storrs, Connecticut 06268*

Synopsis

Electro-copolymerization of methyl acrylate, acrylic acid, methacrylic acid, acrylamide, and methyl methacrylate with acrylonitrile onto graphite fibers has been successfully done in our laboratory. The coatings are relatively uniform and their properties, especially their modulus, can be systematically varied by controlling the monomer ratio in the electrolyte solution. This technique is being used to introduce a ductile interlayer of controlled composition and thickness between the composite fibers and matrix. Copolymers of methyl acrylate and acrylonitrile formed by this technique are random copolymers, with T_g's varying from 10 to 90°C. These copolymers have fairly high molecular weight, in the range of 100,000 g/mol. Monomer reactivity ratios were determined, based upon free radical polymerization kinetics, from cyclic voltammetry. An indirect initiation mechanism is suggested. Bonding between interlayer and matrix can be improved by introducing vinyl monomers with proper functional groups, capable of reacting with the epoxy resin, at the last stage of the electropolymerization process.

INTRODUCTION

High static strength and stiffness, with low density, make graphite-fiber-reinforced epoxy composites particularly attractive for use in weight-critical systems. However, their potential in many structural applications has been hindered to date by the insufficient impact strengths and fracture toughness which they characteristically exhibit.

High strength and stiffness properties of composites require efficient load transfer between fibers and matrix, and thus strong adhesion at the fiber/matrix interface is desired. Various methods have been developed to increase matrix/fiber interfacial bonding.[1] However, the surface treatments which increase the interfacial bonding in brittle-matrix/brittle-fiber composites generally lower the impact and fracture resistances of the composite.[2] Many methods have been proposed and tested to increase the fracture toughness of graphite/epoxy composites, such as the use of a rubber-toughened matrix,[3] a debonding or interlaminar delamination agent,[4,5] hybrid composites,[6,7] and weakened reinforcement.[8] Most of these methods can lead to at least some increase in the energy adsorption on failure, but this is frequently accompanied by a decrease in tensile and flexual properties and difficulty in transferring loads into structures.

For a unidirectional reinforced system, introduction of a ductile interlayer between the fiber and the matrix is expected to improve the fracture toughness and mechanical properties in traverse and off-axis directions without loss of the longitudinal strength, through three major mechanisms discussed below.

First, the interlayer should be able to absorb crack propagation energy and blunt the tip of a crack. It has been recognized from fracture mechanics

Journal of Applied Polymer Science, Vol. 34, 2105–2124 (1987)

CCC 0021-8995/87/062105-20$04.00

that, for homogeneous polymers, the fracture energy is to a large extent dissipated by plastic flow at the crack tip.[9,10] The size of the deformation zone is inversely proportional to the modulus of the material and can be constrained or restrained by dimensions in which this zone is developed.[11] This suggests there is an optimum interlayer thickness which will allow this deformation zone to be fully developed. A larger deformation zone implies higher fracture energy adsorbing capability. A lower modulus interlayer between fiber and matrix will certainly absorb more energy than the rigid matrix and therefore toughen the composite. Also, a large deformation zone will tend to blunt the sharp crack, and more energy will be needed to initiate the crack.[12] Broutman and Agarwal[13] completed a theoretical study which showed that a lower modulus interphase can maximize the composite strain energy release rate without significantly reducing the composite modulus.

Second, the interlayer is capable of relieving the stress concentrations around the reinforcement, present as a result of the curing process or external load. Curing stresses arise from the mismatch of thermal expansion coefficients between matrix and fiber after high temperature curing. For a graphite–epoxy system, the shear stress along the fiber direction will be about 20 MPa. There is also a radial tensile stress of about 3 MPa, and a radial compressive stress of about 14 MPa between any two adjacent fibers, normal to the fiber.[14] The specimen in a prestressed state can be expected to fail at lower load. Kardos suggested that these residual stresses could be relieved by coating the fiber with a material which has a lower modulus than the matrix.[15] Stress concentration can be also induced around the reinforcement from the external load. Marom and Arridge[16] studied the stress patterns of soft interlayers on stainless steel inclusions. Reduction of stress concentration at the interface was observed, and an improvement in the ultimate tensile strength was measured. The surface coating can also separate the fibers from each other—"interface spacing"—and eliminate the exceptionally high stress concentration at the location where fibers contact one another under an applied load.

Third, the interlayer can protect the brittle fiber surface from abrasion during processing, and "heal" the flaws on the fiber surface. It is known that the strength of a high performance fiber is controlled by surface flaws. Fraser et al.[17] believe that the surface damage of high-strength and high-modulus reinforcing fibers such as glass or graphite will result in severe property deterioration and breakage. Good mechanical protection and stress-transfer capability are required for fiber surface coating. By filling the fiber surface flaws with a low modulus material, a crack-healing process can significantly reduce the stress concentration around the surface flaws.[15,18] Both reducing the surface flaw width or increasing the modulus of the interlayer will result in a decrease in the stress concentration about the flaw.

Several kinds of interlayer materials, i.e., epoxy, silicone rubber, poly(divinyl benzene), polyurea, and SBR, have been at least briefly evaluated.[15,18–22] Positive results were reported regardless of the materials employed. However, investigations of the effect of different interlayer properties upon composite properties are not complete. Especially, the thickness and the modulus of the interlayer, which play such important roles in the composite toughening mechanisms, have not been fully investigated.

It is also very difficult to coat individual thin fibers such as graphite with an even thickness interlayer by any sort of conventional dipping process. Carroll has shown that the clam-shell shape liquid drops formed on the fiber represent the equilibrium state even for a liquid with zero contact angle.[23,24] Furthermore, the fibers tend to stick together during processing, especially since commercial fibers are approximately 8 μm in diameter and are sold in bundles of thousands of continuous filaments, which sticking is undesirable for good composite properties.

One promising method for separation of graphite fibers with an even thickness interlayer utilizes the high electrical conductivity of graphite fibers with an electropolymerization technique.[25-27] Subramanian and coworkers have done several electropolymerization and electrodeposition studies as a mean of modifying fiber surface properties,[27-31] with very short polymerization time. By using graphite fibers as an electrode, and by passage of an electrical current through a suitable monomer–electrolyte medium, polymerization occurs on the fiber electrode surface. The electrode acts as the source of the active species which initiates the polymerization.

Three major advantages of electropolymerization are: (1) monomers wet the fiber surfaces more easily than polymers and have lower surface tension, thus providing a more uniform coating than if the polymer were applied directly; (2) several layers with different properties can be applied sequentially; (3) the system is, in principle, easily controlled.

The easiest way to vary the modulus of the polymeric interlayer is to copolymerize a glassy polymer with a rubbery polymer. By varying the composition of the random copolymers formed, different T_g's, corresponding to different modulus at room temperature, can be obtained. Copolymers of methyl acrylate and acrylonitrile formed by the electro-polymerization technique in our labratory are random copolymers and their T_g's vary from 10 to 90°C. That implies the modulus of the copolymers can be varied from 1 MPa to 100 GPa at room temperature. These copolymers will therefore be used as the major interlayers in our future work.

In addition, good chemical bonding between the interlayer and the matrix is very desirable to localize energy dissipation within the interlayer and to transfer the stress to the reinforcement. Effective bonding requires that the interlayer contain functional groups reactive to the epoxy matrix, such as amine, epoxy, or acid groups, which will be able to form chemical bonds with the matrix during crosslinking. This can be attained by copolymerizing a monomer such as glycidyl acrylate, acrylic acid, or acrylamide onto the interlayer surface at the last stage of the polymerization. This glassy outer layer can also reduce the problem of sticking together both in and after removal from the polymerization bath.

EXPERIMENTAL

Materials

Methyl acrylate, acrylonitrile, and methyl methacrylate (Aldrich Chemical Co.) were washed three times with 10% NaOH solution to remove inhibitor, and then several times with distilled water. Final purification was achieved by

TABLE I
Properties of Monomers and Homopolymers

Monomer	Chemical Structure	Solubility in Water (g/100 mL)[32]	Polymer T_g (°C)[33]
Acrylonitrile (AN)	$CH_2{=}CH$ $\vert$ $C{\equiv}N$	7	90
Methyl acrylate (MA)	$CH_2{=}CH$ $\vert$ $C{=}O$ $\vert$ $O{-}CH_3$	5	10
Acrylic acid (AA)	$CH_2{=}CH$ $\vert$ $C{=}O$ $\vert$ $O{-}H$	Very soluble	106
Methacrylic acid (MAA)	$CH_2{=}C{-}CH_3$ $\vert$ $C{=}O$ $\vert$ $O{-}H$	Soluble	501
Acrylamide (AM)	$CH_2{=}CH$ $\vert$ $C{=}O$ $\vert$ NH_2	Very soluble	165
Glycidyl acrylate (GA)	$CH_2{=}CH$ $\vert$ $C{=}O$ $\vert$ $O{-}CH_2{-}CH{-}CH_2$ $\backslash\ /$ O	5	—

distillation under reduced pressure, and the middle fractions were collected and stored under nitrogen. Acylic acid and methacrylic acid were fractionally distilled under reduced pressure before use. Glycidyl acrylate (Polysciences) was used without further purification. Acrylamide (Aldrich Chemical Co.) was crystallized from chloroform at room temperature and dried under vacuum. Table I shows the aqueous solubility and structure of the monomers as well as glass transition temperature of polymers from these monomers. "Fortafil 3" graphite fiber, a PAN-based fiber without pretreatment, was purchased from Great Lakes Chemical Co.

Apparatus

A H-shaped glass cell as shown in Figure 1 was used for electropolymerization. The cell has two compartments, divided by a fine porosity sintered glass disk. The larger compartment was capped with a rubber stopper which helped to position the graphite fiber bundle, reference electrode, nitrogen inlet, and outlet. A Calomel reference electrode was placed near the graphite fibers. A platinum electrode, having a surface area of 2.9 cm^2, was placed in the small compartment and used as counter electrode. The distance between the Pt counter electrode and graphite fiber working electrode was fixed at 6 cm.

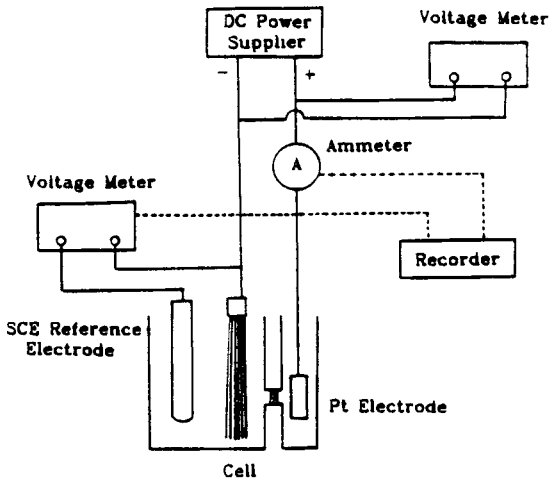

Fig. 1. Schematic diagram of electro-copolymerization batch process.

An "Epsco" Model D-612T filtered DC power supply was used. The graphite fiber bundle was connected as the cathode and the Pt electrode was connected as the anode. Applied voltage and cell current were monitored by a voltameter and ammeter (Fig 1). The potential on the graphite fiber surface was also monitored by the voltage meter against the saturated Calomel (SCE) reference electrode as shown in Figure 1.

Procedure

A 0.05*N* sulfuric acid aqueous solution was prepared, and 100 mL was added to the cell. The solution was purged with nitrogen for 30 min to remove oxygen. A measured amount of monomer mixture was transferred to the cell and mixed until it completely dissolved in the solution, while a nitrogen atmosphere was maintained over the solution surface. A weighed 7 cm long graphite fiber bundle, about 0.5 g, was cut and tied at one end with cotton thread, and then connected to the negative terminal of the power supply through a alligator clip and two copper disks to maintain good contact. The electropolymerization was initiated by passing a current through the solution under a constant applied voltage of 12 v. After 2–3 h (abitrarily selected), the graphite fibers were coated with a thick layer of electropolymerized material. The fiber bundle was withdrawn from the cell, rinsed with distilled water, and then dried in a vacuum oven. The polymer was recovered by extraction with DMF followed by solvent removal under vacuum at 100°C for 24 h.

RESULTS AND DISCUSSION

FTIR Study

Fourier transform IR spectra of the copolymers was used to identify the composition of the copolymers. This was done by the use of a Nicolet 65SX FTIR Spectrophotometer. The infrared absorbances of thin films of the

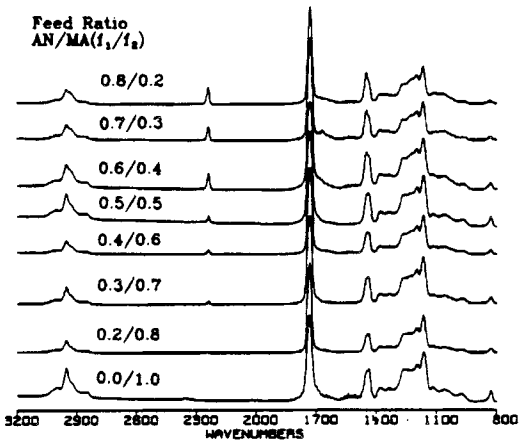

Fig. 2. FTIR spectra of electroinitiated AN/MA copolymers.

AN/MA copolymers from electro-polymerization are shown in Figure 2. The acrylonitrile has a characteristic nitrile peak at 2245 cm^{-1} and methyl acrylate has a characteristic ester carbonyl peak at 1735 cm^{-1}. The absorbance is directly proportional to the concentration of the absorbing component, in accordance with Beer's law. A calibration curve was established by plotting the nitrile/carbonyl peak height ratios with known PAN/PMA blend molar ratios, giving a straight line (Fig. 3). This line was used to determine the composition of the experimental copolymers.

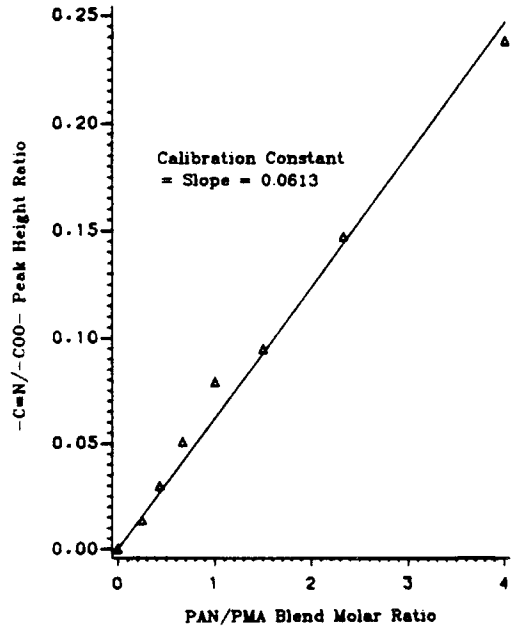

Fig. 3. Composition calibration curve for electroinitiated AN/MA copolymers.

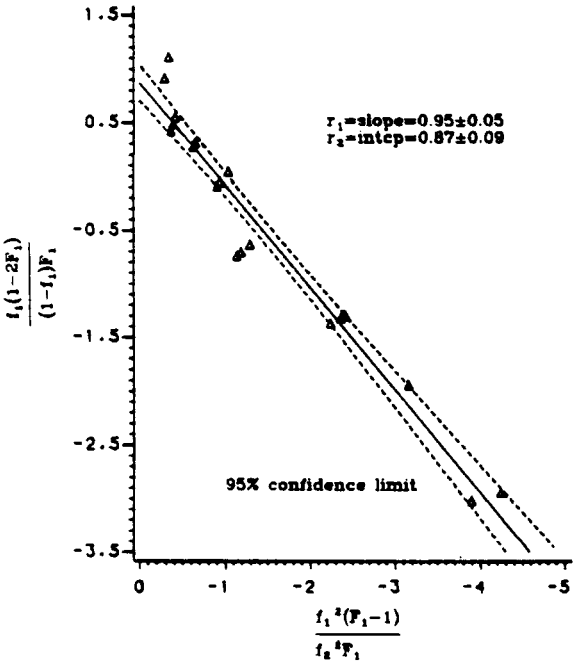

Fig. 4. Determination of monomer reactivity ratios of electroinitiated AN/MA copolymers.

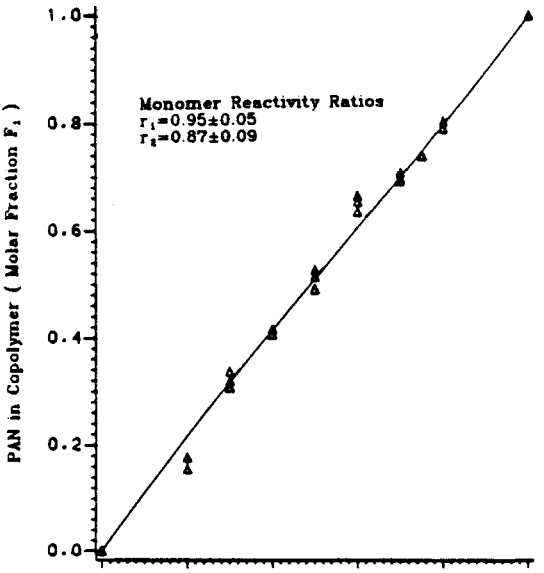

Since less then 5% of monomers in the cell were converted into polymer during the polymerization, the composition of these copolymers can be considered as arising from the initial bath. If one assumes that the reaction proceeds by standard free radical copolymerization kinetics, the monomer reactivity ratios of AN and MA can be determined by rearranging the copolymer equation[34]

$$F_1 = \frac{r_1 f_1^2 + f_1 f_2}{r_1 f_1^2 + 2 f_1 f_2 + r_2 f_2^2}$$

where F is the polymer composition, f is the feed composition, and r is the monomer reactivity ratio into the dimensionless form

$$\frac{f_1(1 - 2F_1)}{(1 - f_1)F_1} = r_2 + \frac{f_1^2(F_1 - 1)}{(1 - f_1)^2 F_1} r_1$$

This equation gives a straight line with slope r_1 and intercept r_2. As shown in Figure 4, the r_1 and r_2 can be determined by the least-square regression of a series of experimental data plotted by Eq. (2). The dashed lines represent the 95% confidence limit, i.e., one can be 95% confident that the regression line shown will fall between two limits. In Figure 5, in which the copolymer composition is plotted against the feed composition, the solid line represents the theoretical interpretation based on the reactivity ratios determined above. The fit is quite good, lending some support to the applicability of free radical copolymerization kinetics to this electro-copolymerization system.

The monomer reactivity ratios determined here are somewhat different from prior measurements reported in the literature, as shown in Table II.[35] This might be due to the different medium, surfactant, and initiator used or might be attributable to an inherent difference associated with electropolymerization. The variation in the prior data is too great for a conclusion to be drawn. However, the electropolymerization data are in the same general range as other data from aqueous systems.

Differential Scanning Calorimeter (DSC) Study

A Omnitherm Q. C. 25 differential scanning calorimeter (DSC) was used to determine the glass transition temperature of the electropolymerized co-

TABLE II
Reported Reactivity Ratios of Acrylonitrile and Methyl Acrylate[35]

r_1	r_2	Temp (°C)	System
0.70 ± 0.20	1.22 ± 0.20	20	Suspension
1.50 ± 0.10	0.84 ± 0.05	50	Benzene
1.26 ± 0.10	0.67 ± 0.10	30	—
1.40 ± 0.10	0.95 ± 0.05	60	Bulk
0.84	0.83	65	Emulsion
0.50 ± 0.05	0.71 ± 0.01	80	—
0.95 ± 0.05	0.87 ± 0.09	23	Electroinitiation[a]

[a] Present work.

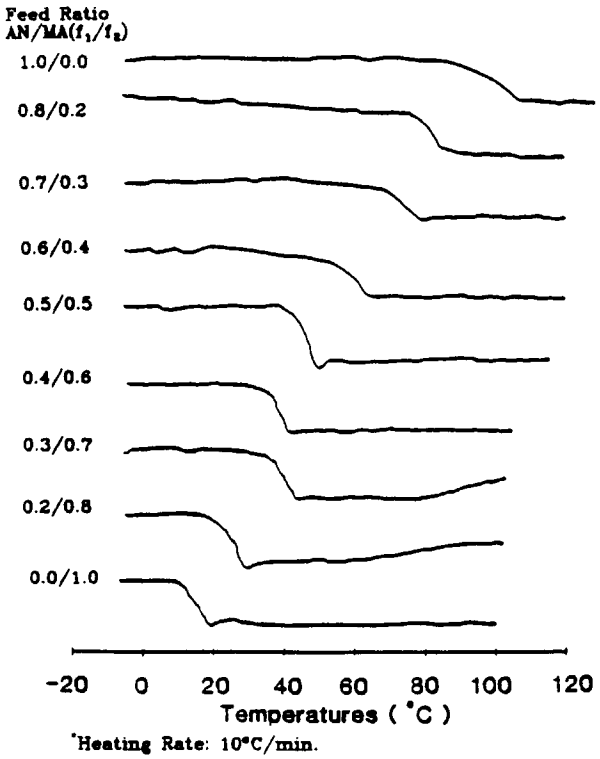

Fig. 6. DSC curves for electroinitiated AN/MA copolymers.

polymers. The DSC curves of the copolymers from different AN/MA feed ratios, collected from the graphite fiber surface, are shown in Figure 6. A 10°C/min heating rate and a sample size of about 15 mg were used. The shift of the baselines corresponds to the glass transition temperature. The T_g of pure poly(methyl acrylate) and polyacrylonitrile are approximately 14 and 98°C, respectively. Only one T_g is observed by DSC for the copolymer samples, which increases as more acrylonitrile is used in the feed. This suggests the copolymers formed on the fiber surface are likely random copolymers and that T_g varies with the composition of the copolymers. The T_g's are plotted against the copolymer composition in Figure 7. The T_g's fall between the Fox equation[36] and Gibbs–DiMarzio equation.[37]

Scanning Electron Microscopy

Scanning electron microscopy was used to investigate the presence and the morphology of electropolymerized material on the surface of the fibers. Gold-sputtered samples were examined with the aid of an AMR 1000A SEM under various magnifications. Scanning electron micrographs of coated graphite fibers from difference AN/MA feed ratios are shown in Figure 8. Figure 8(a) shows untreated graphite fibers, which have a dog-bone-shape cross section. There are three fibers in the photograph. Figure 8(b) is the photograph of fibers treated with pure acrylonitrile. The coating is characteristi-

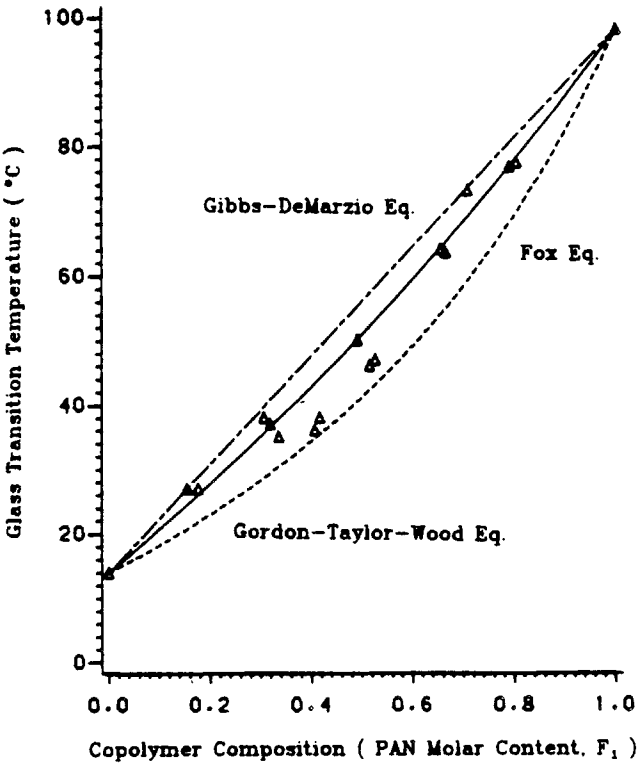

Fig. 7. T_g of AN/MA copolymers vs. composition.

cally "grainy," i.e., the surface appears somewhat like grains of sand bonded together. Polyacrylonitrile polymer exhibits some crystalline polymer properties associated with a unique two-dimensional order.[38] Also, polyacrylonitrile is much less soluble in the polymerization medium, and reduced solubility may contribute to the observed "grainy" structure. Figures 8(c)–8(f) show coated graphite fibers treated with different AN/MA feeds, on which progressively smoother coatings can be observed as the methyl acrylate content is increased. The thickness of these coatings is around 2 μm.

Fibers coated by polymerization of glycidyl acrylate, methacrylic acid, acrylic acid, and acrylamide are also shown in Figure 9. Different morphologies can be seen, which are probably due to the different solubility parameters, wetting characteristics, etc., of the polymers. This is an area for further investigation.

Gel Permeation Chromatography (GPC)

Molecular weight determinations were conducted with the aid of a Waters gel permeation chromatograph, Model 200, equipped with four styragel columns of pore size of 100, 500, 10^3, and 10^4 Å, and with the use of tetrahydrofuran (THF) as the solvent at a flow rate of 1.0 mL/min at 23°C. Only

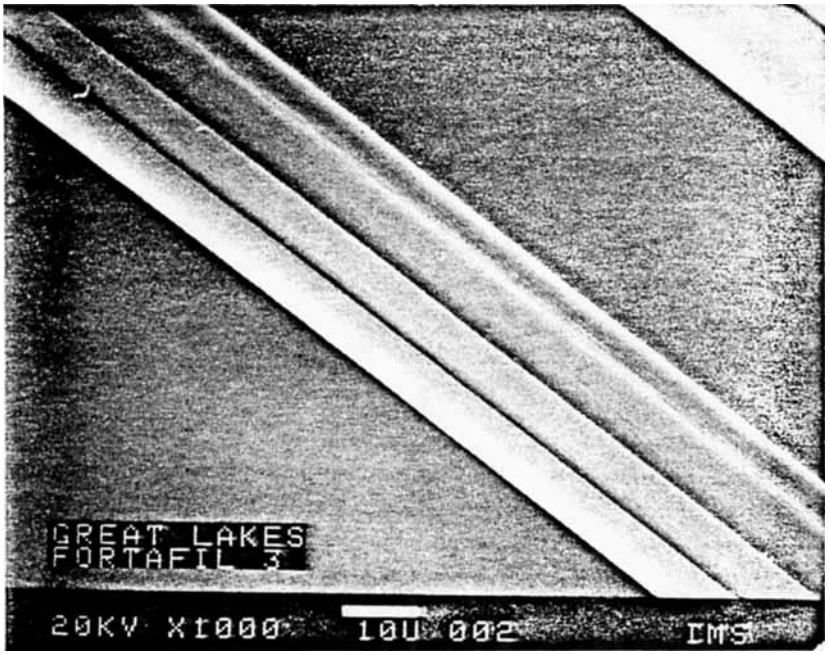

(a)

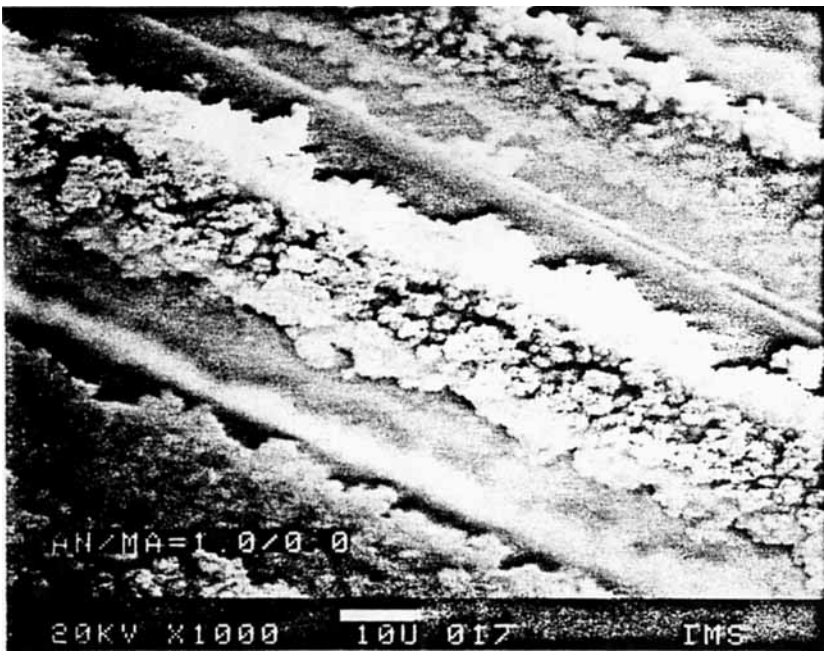

(b)

Fig. 8. SEM micrographs of AN/MA copolymers on graphite fibers: (a) untreated graphite fibers; (b) feed ratio, AN/MA = 1.0/0.0; (c) feed ratio, AN/MA = 0.7/0.3; (d) feed ratio, AN/MA = 0.5/0.5; (e) feed ratio, AN/MA = 0.3/0.7; (f) feed ratio, AN/MA = 0.0/1.0.

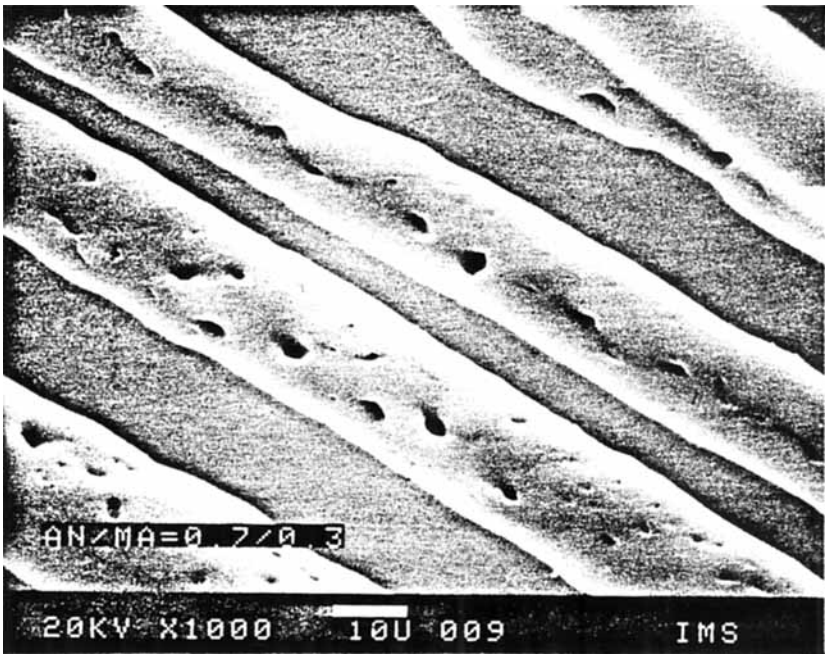

(c)

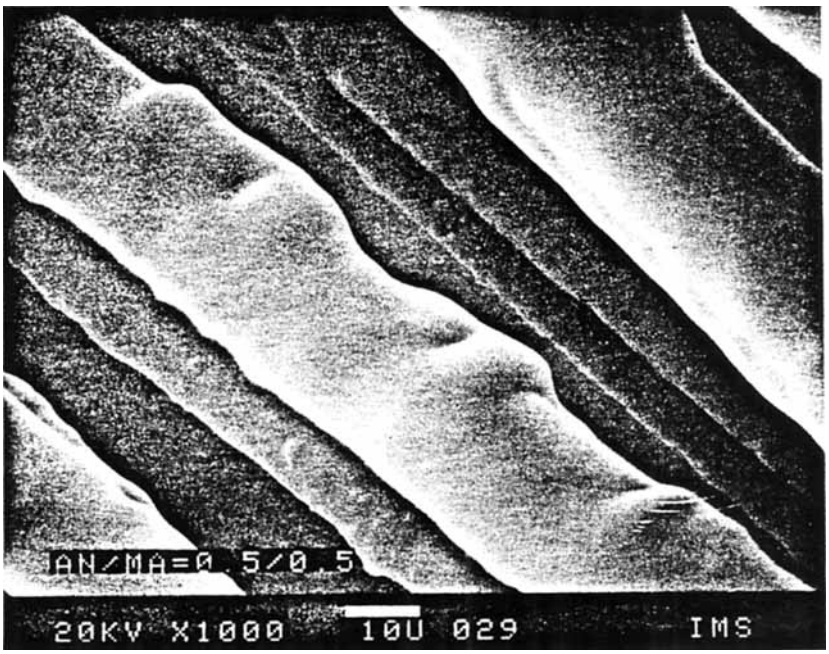

(d)

Fig. 8. (*Continued from the previous page.*)

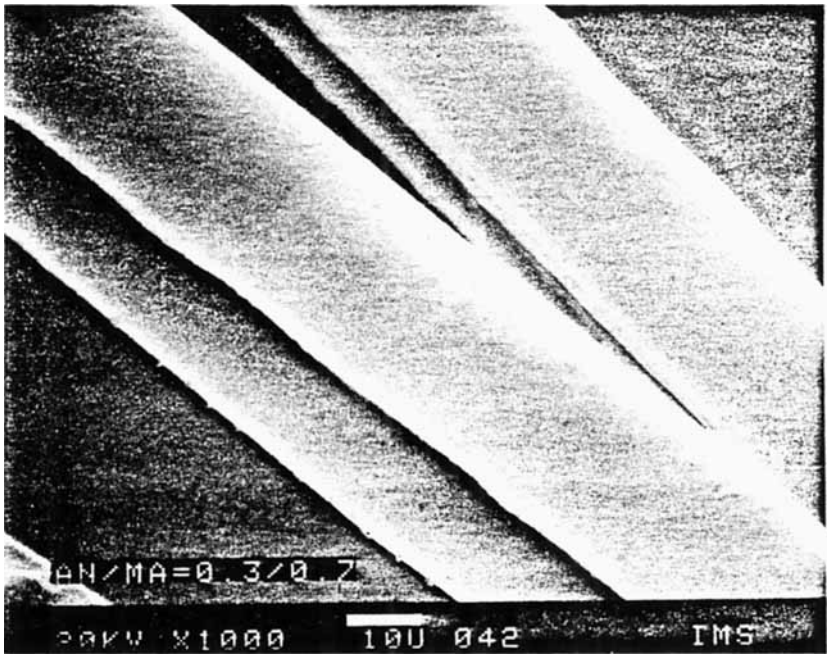

(e)

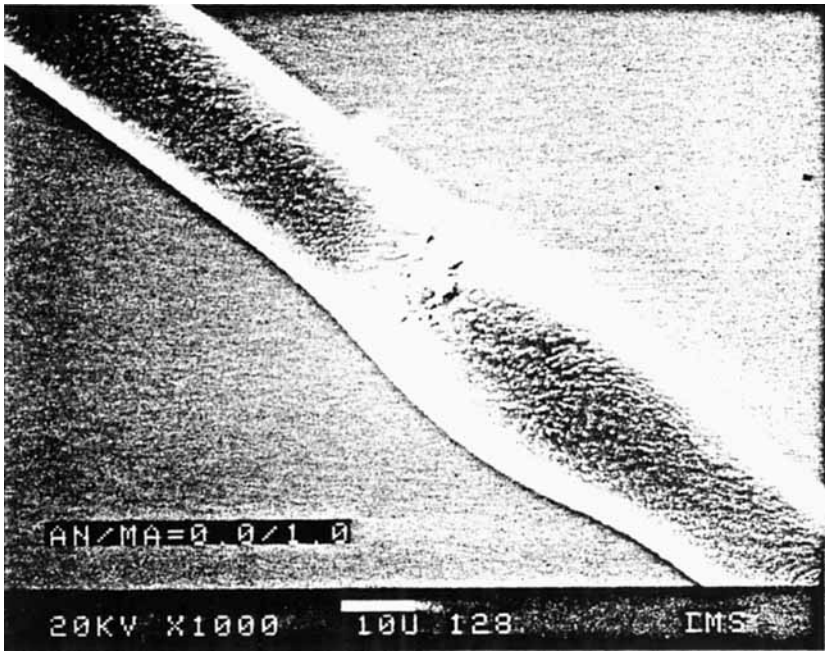

(f)

Fig. 8. (*Continued from the previous page.*)

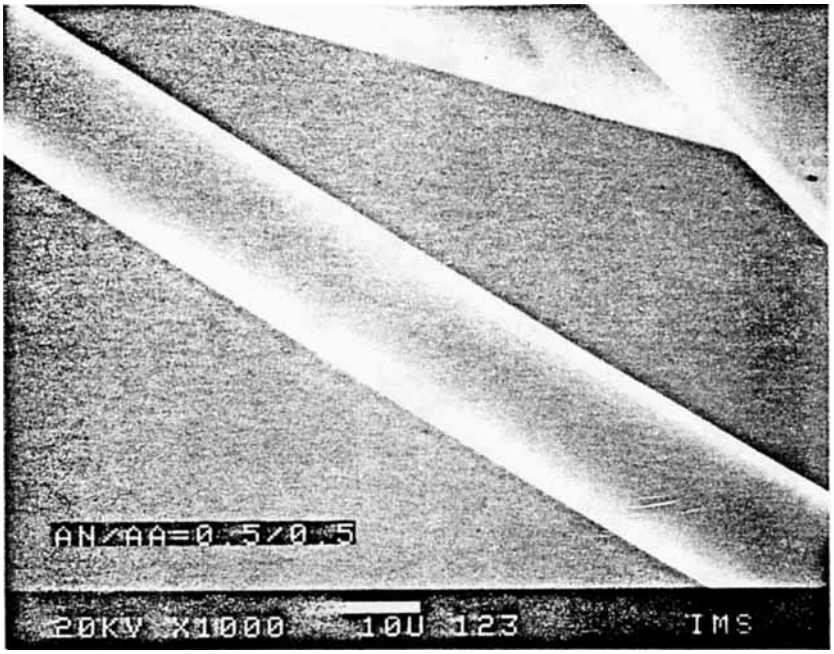

(a)

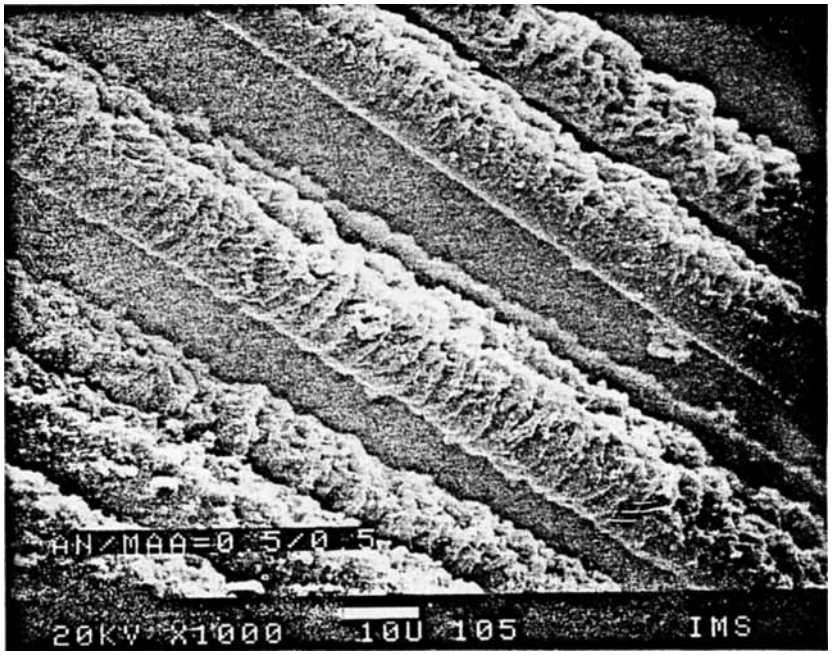

(b)

Fig. 9. SEM micrographs of several polymeric coating on graphite fibers: (a) feed ratio, AN/AA = 0.5/0.5; (b) feed ratio, AN/MAA = 0.5/0.5; (c) feed ratio, AN/AM = 0.5/0.5; (d) feed ratio, AN/GA = 0.5/0.5.

(c)

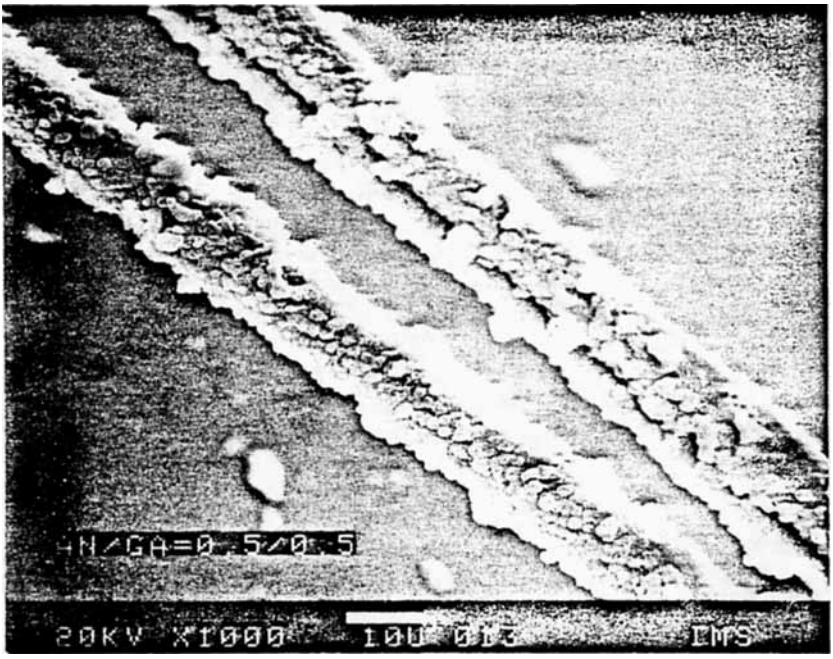

(d)

Fig. 9. (*Continued from the previous page.*)

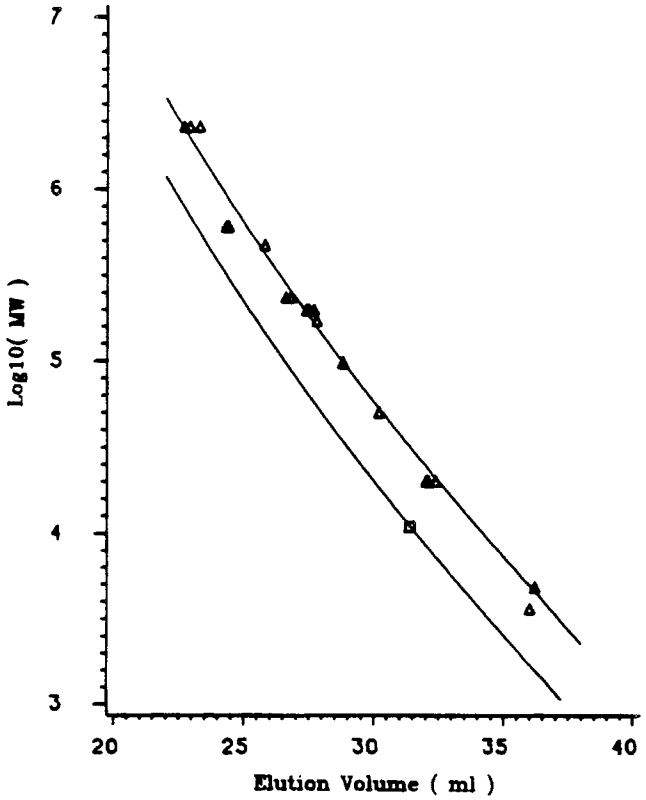

Fig. 10. GPC calibration curve: (△) polystyrene standards; (□) poly(methyl acrylate) standard.

copolymers of low acrylonitrile content, which were therefore soluble in THF, were examined.

Narrow MWD polystyrene standards were used to construct the molecular weight calibration curve (Fig 10). However, the determination of Mark–Houwink constants, K and a, of these copolymers of different composition was not feasible. Since only copolymers with low acrylonitrile content were examined, the Mark–Houwink constants of poly(methyl acrylate (PMA) were used to determine the molecular weight. This is done by shifting the PS calibration curve against the known MW of a pure PMA standard. This corresponds to the lower curve in the Figure 10. The results are shown in Table III. The differences are likely due to irreproducible conditions (fiber contact, etc.) in the polymerization runs, rather than to the monomer ratio.

Cyclic Voltammetry

The presence of the electric current in the monomer's solution is a critical criterion for the polymerization. When the standard experimental procedure was followed but without passing the current through, no polymer was produced. A typical fiber surface potential and cell current change during the polymerization as shown in Figure 11. The current decreases when the

TABLE III
Molecular Weights of Electroinitiated AN/MA Copolymers

Monomer feed molar ratio (AN/MA)	Copolymer composition	($M_n \times 10^5$)	($M_w \times 10^5$)	M_w/M_n
0.0/1.0	0.0/1.0	0.64	2.51	3.92
0.2/0.8	0.17/0.83	1.25	2.76	2.21
0.3/0.7	0.32/0.68	0.52	1.63	3.14
0.4/0.6	0.41/0.59	1.11	2.73	2.47

polymer starts to form on the fiber surface, which acts as an insulating layer and increases the resistance of the cell circuit, thus lowering the current density. The potential on the graphite fiber surface becomes more negative, and the potential drop between the graphite fiber and SCE reference electrode also increases.

Low current density and an extremely low efficiency of the initiation mechanism have proved to have the advantage of placing an even thickness coating on the fiber surface. This is essentially same as the "microthrowing power" technique used in the electroplating industry.[39] Because the polymerization rate is much slower than the monomer transportation rate, the local monomer concentration between the fibers will be approximately same as in the bulk solution.

Cyclic voltammetry was used to measure the reduction potential of the methyl acrylate and acrylonitrile on the graphite fibers and to determine the initiation mechanism. Two systems, one aqueous and the other nonaqueous, containing the monomer were studied. The aqueous system contained 0.05N sulfuric acid as the supporting electrolyte, with 5.0 wt % monomer completely dissolved in the solution. A SCE reference electrode and 100 mV/s cathodic sweep rate was used. Monomers such as methyl acrylate, acrylonitrile, and

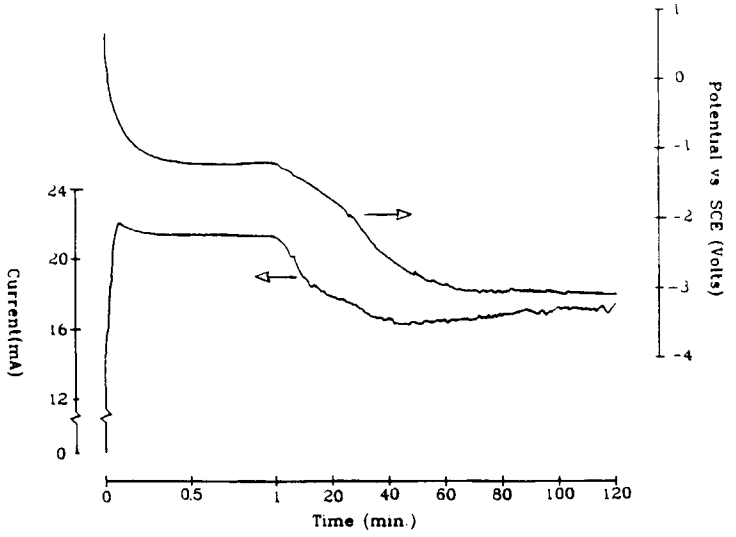

Fig. 11. Current and potential change in electropolymerization.

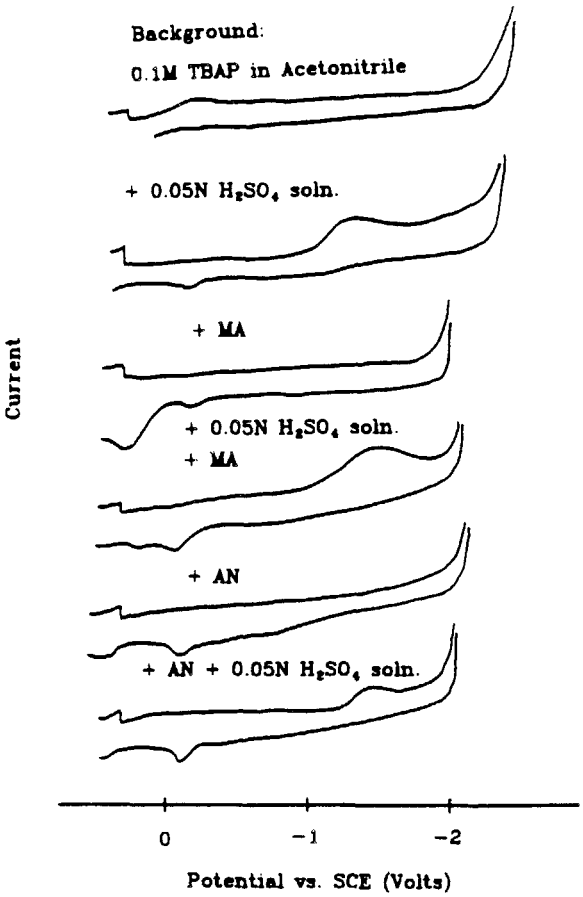

Fig. 12. Cyclic voltammetry of monomers in nonaqueous systems.

glycidyl acrylate were examined. However, the current–potential curves were all found to be the same, within experimental error. A typical aqueous acid electrochemical reaction curve was found,[40] and the only reaction observed was the reduction of solvent/electrolyte. No reduction reaction of monomers was found before the aqueous solvent began to decompose. Since water and acid were present at very high concentration, the current rose sharply and this obliterated observation of any other electrochemical reactions.

Acetonitrile and tetrabutyl ammonium perchlorate (TBAP, 0.1*M*) were used as the solvent and supporting electrolyte in the nonaqueous system. The reference electrode consisted of silver and silver nitrate (0.1*M*) dissolved in the same solvent system as above. A cathodic sweeping rate of 100 mV/s was employed. The current–potential curves of tests for the different monomers are shown in Figure 12. Again, the hydrogen ion reduction peak was the only reaction observed. No acrylonitrile or methyl acrylate reduction peak was found before reaching the working boundary.

From the above observations, we can see that the reduction potentials of these monomers under these condition are higher than the reduction of

hydrogen ions, $H + + e - \rightarrow H \cdot$. It is suggested here that this reaction will indirectly initiate the polymerization in our aqueous polymerization bath. The hydrogen free radicals will react the monomers to start the chain reaction, which initiation process is in competition with recombination of hydrogen free radicals to form hydrogen gas molecules. This suggested that chains are not initiated ionically, since the electrochemical reaction of lowest potential will dominate the entire reaction and the potential can not exceed the boundary limit in the aqueous system. The difficulty of reaction between hydrogen free radicals with monomers may be the reason for the relatively slow polymer formation rate on the fiber surface.

CONCLUSIONS

Thick, high molecular weight copolymers of several monomers have been successfully applied onto the surface of commercial graphite fibers by an electro-copolymerization technique. Even thickness coatings are obtained. Copolymers of acrylonitrile and methyl acrylate were studied in greater detail. The copolymer composition can be controlled by the ratio of monomers in the solution, with their T_g's following the behavior expected from random copolymers. The monomer reactivity ratios determined are somewhat different from other data in the literature based on the free radical polymerization mechanism, although there are within the overall range of values reported. The initiation step is suggested to be the reduction of the protons in the solution to hydrogen radicals, which start the polymerization indirectly. This electrochemical polymerization technique will be used to place an interlayer at the fiber/matrix interface to study the effects upon composite properties.

The authors gratefully acknowledge the financial support of the National Science Foundation (Grant No. CPE-8412480) in this research.

References

1. J. Delmonte, *Technology of Carbon and Graphite Fiber Composites*, Van Nostrand Reinhold, New York, 1981, Chap. 6.
2. L. T. Drzal, M. J. Rich, J. D. Camping, and W. J. Park, Proc. 35th SPI RP/C Conf., 1980, Sec. 20C.
3. C. Keith Riew and J. K. Gillham, Ed., *Rubber-Modified Thermoset Resins*, ACS 208, American Chemical Society, Washington, DC, 1984.
4. A. G. Atkins, *J. Mater. Sci.*, **10**, 819–832 (1975).
5. J. P. Farve, *J. Mater. Sci.*, **12**, 43–50 (1977).
6. D. F. Adams and A. K. Miller, *Mater. Sci. Eng.*, **19**, 245–260 (1975).
7. J. Summerscales and D. Short, *Composites*, **9**(3), 157–166 (1978).
8. G. A. Cooper, *J. Mater. Sci.*, **5**, 645–654 (1970).
9. A. J. Kinloch, *Metal Sci.*, (Aug.-Sep.), 305–318 (1980).
10. B. W. Cherry, and K. W. Thomson, *J. Mater. Sci.*, **16**, 1913–1924 (1981).
11. A. J. Kinloch and S. J. Shaw, *J. Adhesion*, **12**, 59–77 (1981).
12. A. J. Kinloch and J. G. Williams, *J. Mater. Sci.*, **15**, 987–996 (1980).
13. L. J. Broutman and B. D. Agarwal, *Polym. Eng. Sci.*, **14**(8), 581–588 (1974).
14. D. A. Scola, *Composite Materials, Vol. 6, Interface in Polymer Matrix Composites*, E. P. Pludemann, Ed. Academic, New York, 1974.
15. L. D. Tryson and J. L. Kardos, Proc. 36th SPI RP/C Conf., Feb. 1981, Sec. 2-E.
16. G. Marom and R. G. C. Arridge, *Mater. Sci. Eng.*, **23**, 23–32 (1976).

17. W. A. Fraser, F. H. Ancker, A. T. DiBenedetto, and B. Elbirli, *Polym. Composite*, 4(4), 238–248 (1983).
18. R. E. Lavengood and M. J. Michno Jr., Monsanto Research Corp., Report AD-776-592, 1974.
19. N. L. Hancox and H. Wells, *Fiber Sci. Technol.*, **10**, 9–22 (1977).
20. E. B. Trostyanskaya and L. P. Kobets, *Plast. Massy.*, **1**, 53–56 (1970).
21. J. H. Cranmer, G. C. Tesoro, and D. R. Uhlmann, *Ind. Eng. Chem., Proc. Res. Dev.*, **21**, 185–190 (1982).
22. E. P. Plueddemann, Proc. 29th SPI RP/C Conf., 1974, Sec. 24-A.
23. B. J. Carroll, *J. Colloid Interface Sci.*, **57**(3), 488–495 (1976).
24. B. J. Carroll, *J. Colloid Interface Sci.*, **97**(1), 195–200 (1984).
25. J. R. MacCallum and D. H. MacKerron, *Br. Polym. J.*, **14**(3), 14–18 (1982).
26. J. R. MacCallum and D. H. MacKerron, *Eur. Polym. J.*, **18**, 717–724 (1982).
27. R. V. Subramanian and J. J. Jakubowski, *Polym. Eng. Sci.*, **18**(7), 590–600 (1978).
28. R. V. Subramanian, *Adv. Polym. Sci.*, **33**, 33–58 (1979).
29. J. J. Jakubowski and R. V. Subramanian, *Polym. Bull.*, **1**, 785–791 (1979).
30. R. V. Subramanian, *Pure Appl. Chem.*, **52**(7), 1927–1937 (1980).
31. R. V. Subramanian and S. Own, *Polym. Prepr.*, **22**(2), 203–204 (1983).
32. M. Windholz, Ed., *The Merck Index*, 9th ed., Merck, Rahway, NJ, 1976.
33. J. Brandrup and E. H. Immergut, Eds., *Polymer Handbook*, Wiley, New York, 1975.
34. M. Fineman and S. D. Ross, *J. Polym. Sci.*, **5**, 269 (1950).
35. G. E. Ham, Ed., *Copolymerization*, Wiley, New York, 1964, p. 566.
36. T. G. Fox, *Bull. Am. Phys. Soc.*, 1, 123 (1956).
37. J. H. Gibbs and E. A. DiMarzio, *J. Chem. Phys.*, **28**, 373 (1958).
38. C. R. Bohn, J. R. Schaefgen, and W. O. Statton, *J. Polym. Sci.*, **55**, 531 (1961).
39. O. Kardos, 60th Annual Tech. Conf., Am. Electro. Soc., Minneapolis, MN, June 1973.
40. H. R. Thirsk and J. A. Harrison, *A Guide to Study of Electrode Kinetics*, Academic, London, 1972.

Received June 19, 1986
Accepted September 23, 1986